

Numerical model for time-dependent fracturing of concrete structures and its applications

G. Di Luzio & L. Cedolin

Department of Structural Engineering, Politecnico di Milano, Milano, Italy

ABSTRACT: A constitutive law which incorporates creep and fracture behavior for the analysis of time-dependent cracking of concrete structures is briefly presented. The constitutive model is composed of two parts acting in series: a Maxwell chain for the creep of uncracked concrete and a recent version of the microplane model (M4), which includes the rate-dependence of fracturing associated with the activation energy of bond ruptures, for the cracking. The proposed formulation is applied to the simulation of the size effect of single notched specimens in direct tension for quasi-static fracture in the time domain with different loading rates. The numerical results reveal clearly the link between the size of the fracture process zone (FPZ) and the rate loading.

1 INTRODUCTION

The load carrying capacity of a concrete structure under sustained constant load can be considerably smaller with respect to that of the same structure instantaneously loaded. This can be explained by the interaction between cracking and creep, which may lead to an increase of damage with a reduction of the ultimate load capacity. Moreover, it is well-known that fracture propagation is rate-sensitive, due to the fact that the rupture of interatomic or intermolecular bonds is a thermally activated process (Bažant 1995). Wu & Bažant (1993) used the activation energy process of bond ruptures in order to capture the strength increase with loading rate in a wide range of quasi-static loading rates.

In the last years a significant progress has been made in the modeling of fracture and damage of cementitious materials. To understand and model the creep rupture of concrete different approaches can be found in the literature (among others Bažant 1992, Bažant & Jiràsek 1993, van Zijl et al. 2001, Zhou & Hillerborg 1992, Zhang & Karihaloo 1992, Carpinteri et al. 1995).

In the present paper two different sources of time-dependence in concrete have been considered, a rate dependence of crack propagation, introduced in a three-dimensional constitutive model for concrete such as the microplane model M4, and a linear creep model for the prediction of the viscoelastic behavior of uncracked concrete. In the present approach

the non-linear creep of concrete may be regarded as a consequence of the redistribution of stresses due to creep and, related to it, the increase of damage. Both sources of time-dependence (creep and rate-dependence of crack growth) play an important role in the lifetime of the concrete structures. The prediction capability of this model is demonstrated through the experimental data available in the literature (Zhou 1992). Moreover, the effectiveness of the proposed model is demonstrated through the analysis of single notched specimens in direct tension under different loading rates, which reveals clearly the link between the size of the fracture process zone (FPZ) and the rate loading.

2 COMPUTATIONAL MODEL FOR LONG-TERM BEHAVIOR OF CONCRETE

The stress increment over a time step Δt , $\Delta\sigma = \sigma(t + \Delta t) - \sigma(t)$, in a linear visco-elastic material can be written as (Bažant & Wu 1974)

$$\Delta\sigma = \mathbf{D}^{ve} \Delta\epsilon^{ve} + \sigma^* \quad (1)$$

with

$$\mathbf{D}^{ve} = \left[E_0(t^*) + \sum_{n=1}^N \frac{E_n(t^*)\tau_n}{\Delta t} \left(1 - e^{-\frac{\Delta t}{\tau_n}} \right) \right] \mathbf{D} \quad (2)$$

$$\text{and } \sigma^* = - \sum_{n=1}^N \left(1 - e^{-\frac{\Delta t}{\tau_n}} \right) \sigma_n(t) \quad (3)$$

where \mathbf{D} is a dimensionless matrix obtained from the linear elastic stiffness matrix divided by the Young modulus, $\Delta\epsilon^{ve}$ is the visco-elastic strain increment in the time step Δt , $E_n(t^*)$ is the stiffness modulus of the element n , constant in the range $t \leq t^* \leq t + \Delta t$, τ_n is the relaxation time of the element n and $\sigma_n(t)$ is the initial stress in the element n at the time t . The model is equivalent to a Maxwell chain model with time-dependent element stiffnesses which, for example, can be determined through the Solidification Theory (Carol & Bažant 1993).

Assuming the additivity of strains, the strain rate can be expressed as follows

$$\dot{\epsilon} = \dot{\epsilon}^{ve} + \dot{\epsilon}^{cr} + \dot{\epsilon}^{sh} + \dot{\epsilon}^t \quad (4)$$

where $\dot{\epsilon}$ is the total strain rate, $\dot{\epsilon}^{ve}$ is the visco-elastic strain rate, $\dot{\epsilon}^{cr}$ is the cracking strain rate, $\dot{\epsilon}^{sh}$ is the shrinkage strain rate, and $\dot{\epsilon}^t$ is the thermal strain rate. Substituting the strain rate with the strain increment over a finite time step and recalling Equation 1 one gets

$$\Delta\sigma = \mathbf{D}^{ve} \Delta\epsilon^{ve} + \sigma^* = \mathbf{D}^{ve} (\Delta\epsilon - \Delta\epsilon^{cr} - \Delta\epsilon^{sh} - \Delta\epsilon^t) + \sigma^* \quad (5)$$

In the following, shrinkage and thermal strain, which are not essential in the present application, will be disregarded ($\Delta\epsilon^{sh} = \Delta\epsilon^t = 0$).

The evolution of the cracking strain is assumed to be governed by the Microplane Model M4 (Bažant et al, 2000a). This constitutive model has an explicit formulation that gives the stress tensor for a given strain tensor

$$\sigma = f_{M4}(\epsilon^{el-cr}) \quad (6)$$

in which ϵ^{el-cr} is the elastic and cracking deformation and f_{M4} is a function which represents the microplane model formulation. According to Equation 6, the stress increment for a given strain increment $\Delta\epsilon^{el-cr}$ in the time step can be written as

$$\Delta\sigma = f_{M4}(\epsilon^{el-cr} + \Delta\epsilon^{el-cr}) - \sigma^{initial} \quad (7)$$

where $\sigma^{initial}$ is the initial stress at the beginning of the time step. Since the stress increment can be written as $\Delta\sigma = \mathbf{E}\Delta\epsilon^{el}$, the cracking strain increment is

$$\Delta\epsilon^{cr} = \Delta\epsilon^{el-cr} - \mathbf{E}^{-1} [f_{M4}(\epsilon^{el-cr} + \Delta\epsilon^{el-cr}) - \sigma^{initial}] \quad (8)$$

where \mathbf{E} is the linear elastic stiffness matrix. Substituting Equation 8 into Eq. 5 one obtains

$$\Delta\sigma = \mathbf{D}^{ve} [\Delta\epsilon - \Delta\epsilon^{el-cr} + \mathbf{E}^{-1} (f_{M4}(\epsilon^{el-cr} + \Delta\epsilon^{el-cr}) - \sigma^{initial})] + \sigma^* \quad (9)$$

Since the viscoelastic model and the Microplane Model M4 are coupled in series, the viscoelastic stress increment and the Microplane model M4 stress increment must be the same. After some mathematical manipulations Equations 5 and 9 become an equation in the only unknown $\Delta\epsilon^{el-cr}$

$$f_{M4}(\epsilon^{el-cr} + \Delta\epsilon^{el-cr}) - \mathbf{D}^{ve} \mathbf{E}^{-1} f_{M4}(\epsilon^{el-cr} + \Delta\epsilon^{el-cr}) + \mathbf{D}^{ve} \Delta\epsilon^{el-cr} = \mathbf{b} \quad (10)$$

where $\mathbf{b} = \mathbf{D}^{ve} (\epsilon - \mathbf{E}^{-1} \sigma^{initial}) + \sigma^* + \sigma^{initial}$ is a vector of constants in each time step. The previous set of nonlinear equations must be solved iteratively. At a certain iteration i of the solution algorithm the residual is

$$\mathbf{r}(\Delta\epsilon^{el-cr}) = f_{M4}(\epsilon^{el-cr} + \Delta\epsilon^{el-cr}) - \mathbf{D}^{ve} \mathbf{E}^{-1} f_{M4}(\epsilon^{el-cr} + \Delta\epsilon^{el-cr}) + \mathbf{D}^{ve} \Delta\epsilon^{el-cr} - \mathbf{b} \quad (11)$$

Taking a Taylor expansion of the residual about the current value of the elastic-cracking strain, ϵ_i^{el-cr} , dropping the terms which are of higher order than linear in $\Delta\epsilon^{el-cr}$, and setting the resulting residual equal to zero, one obtains a linear system of equations for $\Delta\epsilon^{el-cr}$ which represents the linearized model of the nonlinear equation (11). The proposed linearized model is quite powerful, but it still has the disadvantage of requiring the calculation of the tangent stiffness matrix (Jacobian matrix). To overcome this problem, the initial (elastic) stiffness matrix for the microplane model M4 is employed and the Jacobian matrix becomes equal to the elastic stiffness matrix \mathbf{E} .

In the Newton procedure, the solution of the nonlinear equation is obtained by iteratively solving a sequence of linear models. The new value for the unknown in each step of the iteration is obtained as $\epsilon_{i+1}^{el-cr} = \Delta\epsilon^{el-cr} + \epsilon_i^{el-cr}$ and it is continued until the convergence criterion is met. The convergence criterion used to terminate the iteration is based on the magnitude of the unknown increments $\Delta\epsilon^{el-cr}$.

Using the initial stiffness matrix the convergence to the solution of the iterative procedure is always assured, but it is very slow in the nonlinear regime. Therefore, to accelerate the convergence Broyden's method has been adopted (Press et al. 1996). In the proposed iterative procedure the first three iterations are performed using the Newton procedure with the initial linear stiffness matrix. If the convergence criterion is not met after these three iterations, starting from that point Broyden's method is adopted and the convergence to the solution is obtained in one to two iterations. Once $\Delta\epsilon^{el-cr}$ is known, one can calculate the other unknowns $\Delta\epsilon^{cr}$, $\Delta\epsilon^{ve}$ and $\Delta\sigma$

$$\Delta\sigma = f_{M4}(\epsilon^{el-cr} + \Delta\epsilon^{el-cr}) - \sigma^{initial} \quad (12)$$

$$\Delta\epsilon^{cr} = \Delta\epsilon^{el-cr} - \mathbf{E}^{-1}\Delta\sigma \quad \text{and}$$

$$\Delta\epsilon^{ve} = \Delta\epsilon - \Delta\epsilon^{cr} \quad (13)$$

At convergence the visco-elastic strain tensor is obtained according to Equation 13, which also enables the calculation of the internal stresses of the Maxwell chain elements. For the first element one finds

$$\sigma_0(t + \Delta t) = \sigma_0(t) + \mathbf{D}E_0(t^*)\Delta\epsilon^{ve} \quad (14)$$

while for the others

$$\sigma_n(t + \Delta t) = \sigma_n(t) +$$

$$\left[\mathbf{D} \frac{E_n(t^*)\tau_n}{\Delta t} \Delta\epsilon^{ve} - \sigma_n(t) \right] (1 - e^{-\Delta t/\tau_n}) \quad (15)$$

More details on the proposed formulation can be found in Di Luzio (in prep.).

3 RATE DEPENDENT MICROPLANE MODEL M4

The microplane model is a three-dimensional macroscopic constitutive law for modelling quasi-brittle materials which exhibit softening. In the microplane model the material law is characterized by simple relations between the stress and strain components on planes of various orientations. In the present paper a recent version of the microplane model for concrete, proposed and tested by Bažant and coworkers (Bažant et al. 2000a; Caner & Bažant 2000) called M4, is used. The microplane model M4 has the inelastic behavior characterized on the microplane level by the so-called stress-strain boundaries, which may be regarded as strain-dependent yield limits and exhibit strain softening. The original formulation of the microplane model M4 (Bažant et al. 2000a) has been slightly modified as reported in Bažant et al. (2004) and Di Luzio (in press).

The formulation proposed by Bažant (Bažant 1993, Bažant 1995), in which the rate dependence of a cohesive crack is described by the activation energy theory, is adopted. According to this theory the rate effect dependence is nonlinear. The rate-dependence is introduced in the microplane model M4 as proposed by Bažant et al. (2000b). The macroscopic strain softening function $\sigma = F(\epsilon)$ may be written as

$$F(\epsilon) = F^0(\epsilon) [1 + C_2 \text{asinh}(\dot{\epsilon}/C_1)] \quad (16)$$

$F(\epsilon)$ represents the stress-strain boundary (tensile normal stress; compressive volumetric stresses; tensile and compressive deviatoric stresses; and the cohesion in the friction boundary) on the microplane corresponding to strain rate $\dot{\epsilon}$ and $F_0(\epsilon)$ has the meaning of the static stress-strain boundary that corresponds

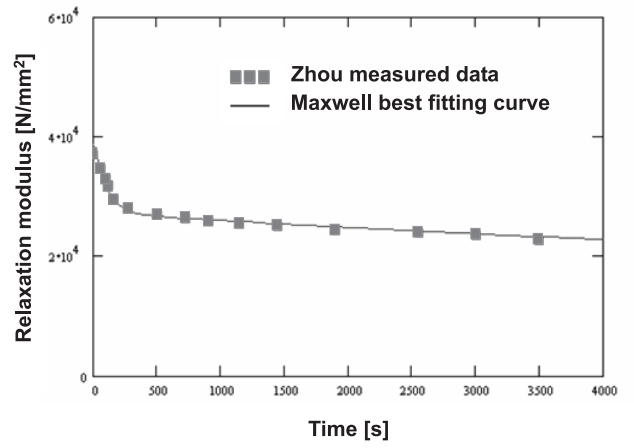


Figure 1: Maxwell chain fit to relaxation data.

to a vanishing strain rate. Equation 16, which transforms the static boundary $F_0(\epsilon)$ to a rate-dependent boundary, represents a vertical scaling of the boundary curve. The rate effect on the frictional yield surface is also applied as a vertical shift of the horizontal asymptote.

It is known that the concept of softening continuum leads to serious problems, i. e. the boundary value problem becomes ill-posed and the numerical calculations cease to be objective, exhibiting pathological spurious mesh sensitivity and unrealistic damage localization. To suppress it and to prevent the damage from localizing into a zone of zero volume, the simplest remedy is to adjust the post-peak slope of the stress-strain diagram as a function of the element size (this was done in the crack band model of Bažant & Oh 1983). This type of localization limiter is adopted in the microplane model M4, in which the microplane limit curves are assumed as functions of the crack band width h . For solid eight node elements the crack band width is assumed to be equal to the average element size $h = V^{1/3}$, where V is the volume of the finite element.

4 NUMERICAL SIMULATIONS OF BENDING TESTS

The experimental investigation of Zhou (1992) has been considered for validating the proposed computational framework. The beams were sealed to avoid shrinkage and subjected to three-point bending tests. Initially the parameters of the microplane model were calibrated on the basis of the mechanical properties of the concrete: Young modulus of 36GPa and tensile strength of 2.8MPa. The parameters of a Maxwell chain model with 7 elements were calibrated through the least square method, by fitting the experimental relaxation curve obtained from cylindrical notched tensile specimens (Fig. 1). Since the relaxation tests were performed over a short time (1 hour) and all of the other tests have a short duration, a non-aging material behavior has been assumed. Zhou

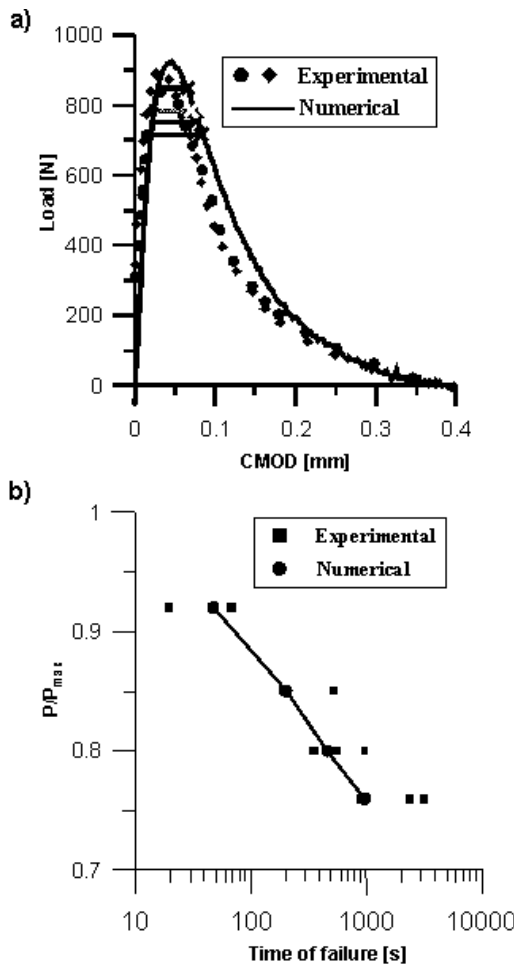


Figure 2: Three-point-bending tests by Zhou (1992): a) load vs deflection curves for different deflection rates; b) time to failure under sustained loads.

(1992) also studied the influence of loading rate on the peak strength through three-point-bending tests under displacement control on smaller beams (cross section of $50 \times 50 \text{ mm}^2$ and length of 600mm) with different deflection rates (from $0.05 \mu\text{ms}^{-1}$ to $50 \mu\text{ms}^{-1}$). To fit these test data the rate parameters were varied in a trial-and-error fashion until a satisfactory agreement was found.

After the calibration of the model parameters, a displacement-controlled three-point-bending test was simulated with a deflection rate of $5 \mu\text{ms}^{-1}$, after which the creep tests were conducted on the same type of specimen by increasing the central force to a predefined level and then sustaining it. Four load levels of 76%, 80%, 85% and 92% of the maximum load capacity of the displacement-controlled case have been considered. The failure in the creep tests occurred in a such a way that the displacement-controlled curve describes very well the failure envelope characterizing the deformation at failure under sustained load. The numerical procedure goes on until equilibrium is no longer ensured for the sustained load level, i.e. the load bearing capacity of the specimen is exceeded. When this happens, the

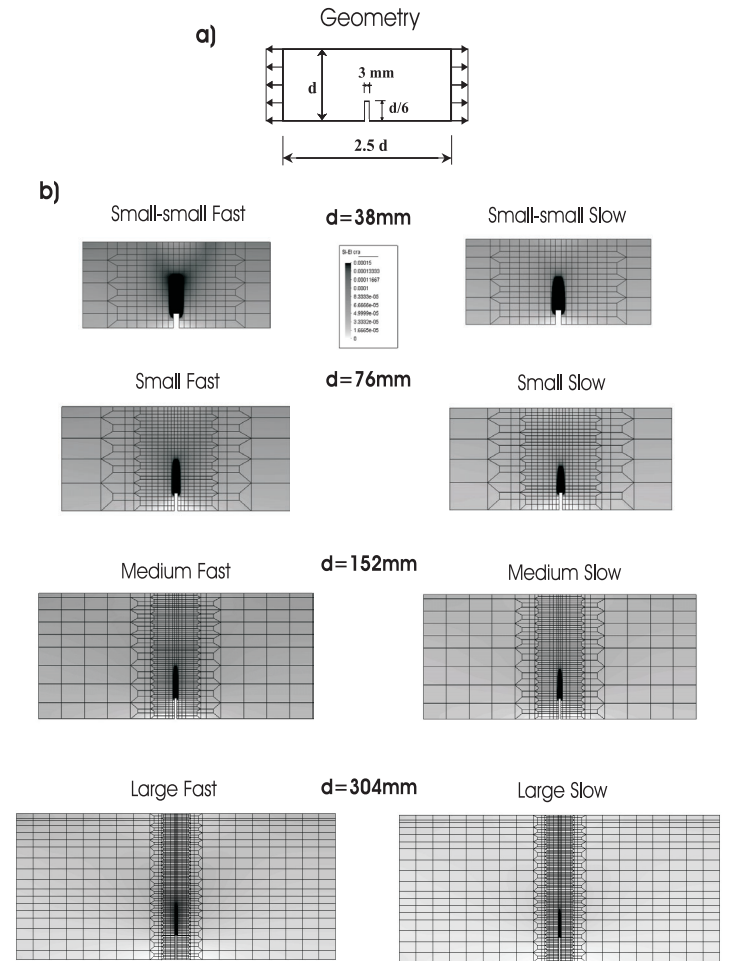


Figure 3: a) Sample geometry of the tensile direct test, b) distribution of the maximum principal cracking strain at the peak for different loading rates and sizes.

Newton-Raphson iterative procedures are no longer able to reach convergence. The numerical results are presented in Figure 2, showing a good agreement with experiments.

5 NUMERICAL ANALYSIS OF SIZE EFFECT TESTS AT VARIOUS LOADING RATES

The proposed computational framework, calibrated on the basis of the experimental data studied in the previous section, has been used to predict the influence of loading rate on geometrically similar specimens. As already pointed out from experimental investigations (Bažant & Gettu 1992), the lower the loading rate the more brittle the fracture propagation, which means that the size effect curve has a significant shift toward the right as the loading rate decreases. This physical phenomenon can be explained by a reduction of the damage distribution (FPZ) as the loading rate decreases.

The direct tensile test has been adopted for these simulations, because a constant crack mouth opening displacement rate can be imposed. Figure 3a shows the specimen geometry. The finite element

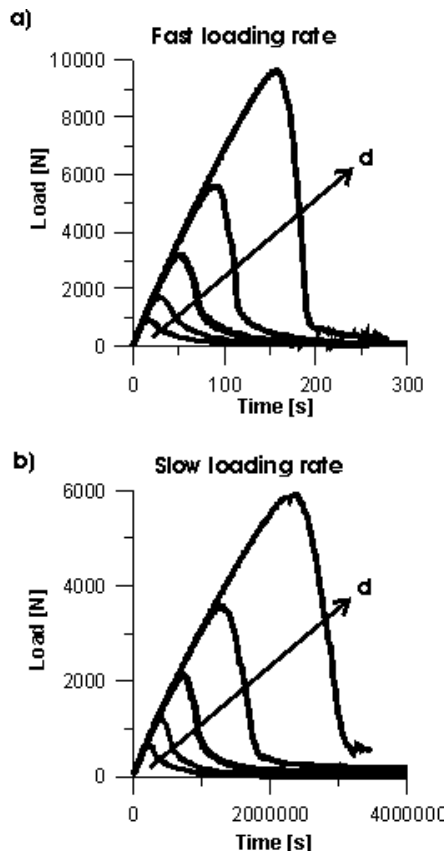


Figure 4: Load versus time for fast (a) and slow (b) loading rates for different sizes (d).

meshes for five different specimen sizes, with size ratio 1:2:4:8:16, are shown in Figure 3b. The smallest specimen depth is $d = 38$ mm, and the largest one is $d = 608$ mm. The thickness is $b = 38$ mm for each size. The specimens were loaded through a constant displacement velocity of 510^{-3} mm/s and of 510^{-8} mm/s for the faster and the slower loading rates, respectively. The maximum principal cracking strain distribution at the peak for different loading rates and sizes is depicted in Figure 3b, which reveals clearly that the damage and the energy dissipation for each size are more spread out for high loading rates. The volume in which the energy is dissipated (FPZ) is reduced for very slow loading rates by the effect of creep. For both fast and slow loading rates, Figures 4a, b report the numerical load versus time curves.

Let us apply now to the results of the numerical simulations (expressed in terms of nominal stress at maximum load $\sigma_N = P_{\max}/db$) Bažant's size effect law (Bažant & Planas 1998):

$$\sigma_N = \frac{\sigma_0}{\sqrt{1 + d/d_0}} \quad (17)$$

in which the constants σ_0 and d_0 can be determined from the numerical (or experimental) results. Rewriting Equation 17 in the plot $Y = (1/\sigma_N)^2$ versus $X = d$, the size-effect-law appears as a straight line $Y = AX + C$ in which $\sigma_0 = 1/\sqrt{C}$ and $d_0 = C/A$.

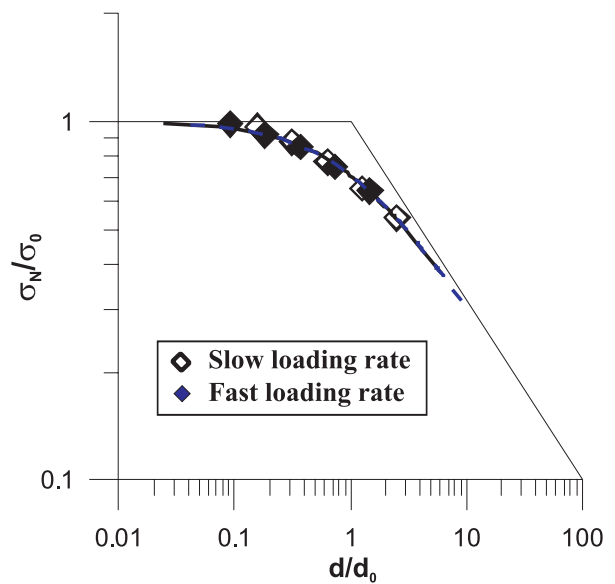


Figure 5: Size effect law (S.E.L.) for fast and slow loading rates. Comparison of the two size effect results with the shift toward the right as the loading becomes slower.

The coefficients A and C have been determined performing a linear regression of Y versus X , getting $A = 4.52510^{-4}$ MPa $^{-2}$ /mm and $C = 0.157$ MPa $^{-2}$ (from which $\sigma_0 = 2.525$ MPa and $d_0 = 346.66$ mm) for the fast series and $A = 1.47610^{-3}$ MPa $^{-2}$ /mm and $C = 0.282$ MPa $^{-2}$ (from which $\sigma_0 = 1.884$ MPa and $d_0 = 191.0$ mm) for the slow series. Figure 5 clearly shows that by reducing the loading rate the size effect curve has a shift toward the right with a change in the mode of failure, i.e. the fracture becomes more brittle as the loading becomes slower. This is confirmation that fracture propagation and the size effect are time dependent processes for concrete.

6 CONCLUSIONS

The microplane model M4 with rate dependence, coupled with a linear viscoelastic element, is capable of predicting the interaction between fracture and creep in concrete. The proposed time-dependent model has been verified for experimental tests of up to 3 hours in duration (Zhou, 1992). It has been shown that the inclusion of both sources of time-dependence, i.e. creep and rate-dependence of crack growth, must be considered to obtain the correct prediction of life expectancy under a constant loads.

The proposed constitutive model is also able to capture the increase of concrete brittleness as the loading rate becomes slower, which appears with a significant shift toward the right (toward LEFM in the size effect plot) as the loading rate decreases. This phenomenon is explained in the numerical simulations with a reduction of the size of the FPZ as the loading rate becomes slower.

ACKNOWLEDGMENT

The authors gratefully acknowledge the financial support of the Italian Department of Education, University and Scientific Research (MIUR) to the project "Calcestruzzi Fibro-rinforzati per Strutture ed Infrastrutture Resistenti, Durevoli ed Economiche".

REFERENCES

- [1] Bažant, Z.P. 1992. Rate effects, size effects and nonlocal concept for fracture of concrete and other quasi-brittle material. *Mechanisms of Quasi-brittle Material*, S. Shah (ed.), Kluwer, Dordrecht, 131-153.
- [2] Bažant, Z.P. 1995. Creep and damage in concrete. *Proc., Materials science of concrete IV*, J. Skalný and S. Mindess, Eds., Am. Ceramic Soc., Westerville, OH, 355-389.
- [3] Bažant, Z.P., Caner, F., Carol, I., Adley, M. & Akers, S.A. 2000a. Microplane Model M4 for Concrete. I: formulation with work-conjugate deviatoric stress. *J. Engrg. Mech.*, ASCE 126, 944-953.
- [4] Bažant, Z.P., Caner, F., Adley, M. & Akers, S.A. 2000b. Fracturing rate effect and creep in microplane model for dynamics. *J. Engrg. Mech.*, ASCE 126, 962-970.
- [5] Bažant, Z.P., Caner, F.C., Cedolin, L., Cusatis, G. & Di Luzio, G. 2004. Fracturing material models based on micromechanical concepts: recent advances. In V.C. Li, C.K.Y. Leung, K.J. Willam, S.L. Billington (eds.), *Fracture Mechanics of Concrete and Concrete Structures - FraMCoS-5, Proc.*, Vail Colorado, 83-89.
- [6] Bažant, Z. P. & Oh, B.-H. 1983. Crack band theory for fracture of concrete. *Mat. and Struct.*, RILEM 16(93), 155-177, Paris.
- [7] Bažant, Z. P. & Gettu, R. 1992. Rate effect and load relaxation in static fracture of concrete. *ACI Mat. J.*, 89(5), 456-468.
- [8] Bažant, Z. P. & Wu, S.T. 1974. Rate-type creep law of aging concrete based on Maxwell chain. *Mat. and Struct.*, RILEM 7, 45-60.
- [9] Bažant, Z.P. & Jiràsek, M. 1993. R-curve modeling of rate and size effects in quasi-brittle material. *Int. J. of Fract.* 62, 355-373.
- [10] Caner, F., and Bažant, Z. P. 2000. Microplane Model M4 for Concrete. II: algorithm and calibration. *J. Engrg. Mech.*, ASCE 126, 954-961.
- [11] Carol, I. & Bažant, Z.P. 1993. Viscoelasticity with aging caused by solidification of nonaging constituent. *J. Engrg. Mech.*, ASCE 119(11), 2252-2269.
- [12] Carpinteri, A., Valente, S., Zhou, F.P., Ferrara, G. & Melchiorri, G. 1995. Crack propagation in concrete specimens subjected to sustained loads. *Fracture Mechanics of Concrete Structures*, Wittmann, F.H. (Ed.), Aedificatio, Germany, 13151328.
- [13] Di Luzio, G. 2007a. A numerical model for concrete time-dependent fracturing. submitted to *J. Engrg. Mech.*, ASCE.
- [14] Di Luzio, G. 2007b. A symmetric over-nonlocal microplane model M4 for fracture in concrete. *Int. J. Solids and Struct.* in press.
- [15] Press, W.H., Teukolsky, W.A., Vetterling, W.T. & Flannery, B.P. 1996. *Numerical Recipes in Fortran 90: the Art of Parallel Scientific Computing*, Cambridge University Press.
- [16] van Zijl, G., de Borst, R. & Rots, J. 2001. A numerical model for the time-dependent cracking of cementitious materials. *Int. J. Num. Met. in Engrg.* 38, 5063-5092.
- [17] Wu, Z.S. & Bažant, Z. P. 1993. Finite element modeling of rate effect in concrete fracture with influence of creep. Z.P. Bažant, I. Carol (eds.), *5th International RILEM Symposium on Creep and Shrinkage of Concrete, Proc.*, London, U.K., 427-432.
- [18] Zhang, C. & Karihaloo, B. 1992. Stability of crack in linear visco-elastic tension softening material. *Proc., Fracture Mechanics of Concrete Structures*, Z.P. Bažant (ed.), Elsevier Applied Science, The Netherlands, 75-81.
- [19] Zhou, F.P. & Hillerborg, A. 1992. Time-dependent fracture of concrete: testing and modelling. *Proc., Fracture Mechanics of Concrete Structures*, Z.P. Bažant (ed.), Elsevier Applied Science, The Netherlands, 75-81.
- [20] Zhou, F.P. 1992. *Time-dependent crack growth and fracture in concrete*, PhD thesis, Lund University of Technology, Sweden.